



HAL
open science

Monte-Carlo simulation results in estimating a pure-jump Cox-Ingersoll-Ross process

Elise Bayraktar

► **To cite this version:**

Elise Bayraktar. Monte-Carlo simulation results in estimating a pure-jump Cox-Ingersoll-Ross process. 2024. hal-04458194

HAL Id: hal-04458194

<https://hal.science/hal-04458194>

Preprint submitted on 14 Feb 2024

HAL is a multi-disciplinary open access archive for the deposit and dissemination of scientific research documents, whether they are published or not. The documents may come from teaching and research institutions in France or abroad, or from public or private research centers.

L'archive ouverte pluridisciplinaire **HAL**, est destinée au dépôt et à la diffusion de documents scientifiques de niveau recherche, publiés ou non, émanant des établissements d'enseignement et de recherche français ou étrangers, des laboratoires publics ou privés.

Monte-Carlo simulation results in estimating a pure-jump Cox-Ingersoll-Ross process

Elise Bayraktar¹

¹LAMA UMR8050

Univ Gustave Eiffel, Univ Paris Est Creteil, CNRS

F-77447 Marne-la-Vallée, France e-mail: elise.bayraktar@univ-eiffel.fr

Abstract: We consider a pure-jump stable Cox-Ingersoll-Ross (α -stable CIR) process driven by a non-symmetric stable Lévy process with jump activity $\alpha \in (1, 2)$, for which estimators of the drift, scaling and jump activity parameters from high-frequency observations of the process on a fixed time period have been proposed in previous work [1]. We first present a numerical scheme to simulate this process. Next, we describe the challenge presented by the non-symmetric stable Lévy process when computing its density and its derivatives. We finally implement the estimators and carry out simulations to show good estimation accuracy.

Keywords and phrases: Lévy process, Stable process, Cox-Ingersoll-Ross process, Parametric inference, Estimating functions, Monte-Carlo simulations.

February, 14 2024

Introduction

Many fields such as finance and neurosciences use models based on stochastic equations with jump. When modelling interest rates, this led to an extension of the classical Cox-Ingersoll-Ross process (CIR process) introduced in [4] to the α -stable CIR processes (see Jiao et al. [6] and [7]) described by

$$X_t = x_0 + at - b \int_0^t X_s ds + \sigma \int_0^t \sqrt{X_s} dB_s + \delta \int_0^t X_s^{1/\alpha} dL_s^\alpha \quad t \geq 0$$

where $(B_t)_{t \geq 0}$ is a standard Brownian motion and $(L_t^\alpha)_{t \geq 0}$ a non-symmetric α -stable Lévy process with $\alpha \in (1, 2)$. We assume that the characteristic function of L_1^α is given by

$$\mathbb{E}(e^{izL_1^\alpha}) = \exp\left(-|z|^\alpha \left(1 - i \tan \frac{\pi\alpha}{2} \operatorname{sgn}(z)\right)\right).$$

From Theorem 14.15. in Sato [14], such a process is strictly self-similar ie $L_t^\alpha \stackrel{\mathcal{L}}{=} t^{1/\alpha} L_1^\alpha$. We denote by φ_α the density of L_1^α .

This paper follows previous work [1], which focused on the estimation of the drift parameters a and b , the scaling parameter δ and the jump activity α from high-frequency observations of the process on a fixed time period $[0, T]$. The estimation of the drift on a finite time interval is not feasible in the presence of a Brownian motion, so we considered a pure-jump α -stable CIR process ($\sigma = 0$ in the previous equation)

$$dX_t = (a_0 - b_0 X_t) dt + \delta_0 X_t^{1/\alpha_0} dL_t^{\alpha_0}, \quad X_0 = x_0 > 0 \quad (0.1)$$

with $a_0 > 0$, $b_0 \in \mathbb{R}$, $\delta_0 > 0$. We know from Fu and Li [5] that (0.1) admits a strong solution and that this solution is positive.

The estimation proposed in [1] is based on estimating equations. We build a quasi-likelihood by approximating the conditional distribution of X_{t+h} given X_t by the stable distribution appropriately centered and rescaled (see Masuda [10] and Clément and Gloter [3]). We also use the power variation method described by Todorov [15] to build non-rate optimal estimators, then correct them using the one-step method. The one-step method was described by Masuda [11] for the estimation of Ornstein-Uhlenbeck type processes. Brouste and Masuda [2] also used the one-step improvement for a stable Lévy process. We notice that the previous

study [2] was conducted for a symmetric Lévy. In this paper, we are concerned with a non-symmetric Lévy process. Numerically, this makes the computation of the density and its derivatives harder, and the one-step correction more difficult to implement.

The paper is organised as follows. Section 1 presents the numerical scheme used to simulate the process that solves (0.1). Section 2 describes the challenge presented by the computation of the density of the non-symmetric stable Lévy process and its derivatives. Section 3 recalls the estimation method proposed in [1] as well as the asymptotic properties of estimators. Next, we describe in this section how to build the estimators in practice and we confirm numerically the theoretical convergences.

1. Simulating the process

1.1. Numerical scheme

We want to generate the process $(X_t)_{t \in [0,1]}$ that solves equation (0.1) by using a discretisation scheme. We know that the solution X is positive with the choice of parameters $a_0 > 0$ and $\delta_0 > 0$, we therefore want a scheme that preserves this positivity. We use the discretisation scheme proposed by Li and Taguchi [8]. For technical reasons, this scheme uses a truncation and considers a bounded jump coefficient, as the authors were not able to prove consistency without a truncated jump coefficient. Denoting by X_t^H the solution of

$$dX_t^H = (a_0 - b_0 X_t^H)dt + \delta_0 h(X_{t-}^H) dL_t^{\alpha_0}, \quad X_0^H = x_0 > 0$$

where $h(x) = \min\{|x|^{1/\alpha_0}, H\}$ for some arbitrarily large constant $H > 1$, they consider the following positivity preserving scheme : $X_0^{H,n} = x_0$ and for $i \geq 0$

$$X_{\frac{i+1}{n}}^{H,n} = \frac{|X_{\frac{i}{n}}^{H,n} + \frac{a_0}{n} + \delta_0 h(X_{\frac{i}{n}}^{H,n}) \Delta_i^n L^{\alpha_0}|}{(1 + \frac{b_0}{n})}. \quad (1.1)$$

Assuming $\alpha_0 \in (\sqrt{2}, 2)$, they get in Corollary 2.9. a strong rate of convergence. For any $p \in (0, \alpha_0^2 - 2)$, setting $H = n^l$ for $l = \frac{(2/\alpha_0 - 1)/(4\alpha_0)}{1+p(1-\alpha_0/2)}$, there exists $C_{T,p} > 0$ such that

$$\sup_{t \leq T} \mathbb{E}(|X_t - X_t^{n^l, n}|) \leq C_{T,p} n^{-L} \quad (1.2)$$

where $L = (2/\alpha_0 - 1)/(4\alpha_0) - l$ and $C_{T,p}$ converges to infinity as p increases to $\alpha_0^2 - 2$. In practice, $H = n^l$ leads to a very large H for the values of n that we will use (n will be larger than 100 000), hence we will use $H = +\infty$ which corresponds to no truncation or $h(x) = |x|^{1/\alpha_0}$.

1.2. Generation of a α -stable random variable

The previous discretisation scheme relies on simulating the independent increments of the Lévy process $\Delta_i^n L^{\alpha_0} = L_{\frac{i}{n}}^{\alpha_0} - L_{\frac{i-1}{n}}^{\alpha_0} \stackrel{\mathcal{L}}{=} L_{1/n}^{\alpha_0}$. Using the self-similarity property of $(L_t^{\alpha_0})_{t \in [0,1]}$, we know that $\Delta_i^n L^{\alpha_0} \stackrel{\mathcal{L}}{=} n^{-1/\alpha_0} L_1^{\alpha_0}$. Therefore, we only need to simulate independent copies of $L_1^{\alpha_0}$. We use the method presented in Weron [17] to generate $L_1^{\alpha, \beta}$ a α -stable random variable, $\alpha \in (0, 2)$ and $\alpha \neq 1$, of skewness parameter $\beta \in [-1, 1]$, with characteristic function

$$\Phi^{\alpha, \beta}(z) = \mathbb{E} \left(e^{iz L_1^{\alpha, \beta}} \right) = \exp \left(-|z|^\alpha \left(1 - i\beta \tan \left(\frac{\pi\alpha}{2} \right) \operatorname{sgn}(z) \right) \right). \quad (1.3)$$

This method is based on the simulation of V a uniform random variable on $(-\frac{\pi}{2}, \frac{\pi}{2})$ and an independent exponential random variable W with mean 1. Using these variables, we get a α -stable random variable $L_1^{\alpha, \beta}$ by

$$L_1^{\alpha, \beta} = S_{\alpha, \beta} \times \frac{\sin(\alpha(V + B_{\alpha, \beta}))}{(\cos(V))^{1/\alpha}} \times \left(\frac{\cos(V - \alpha(V + B_{\alpha, \beta}))}{W} \right)^{(1-\alpha)/\alpha}, \quad (1.4)$$

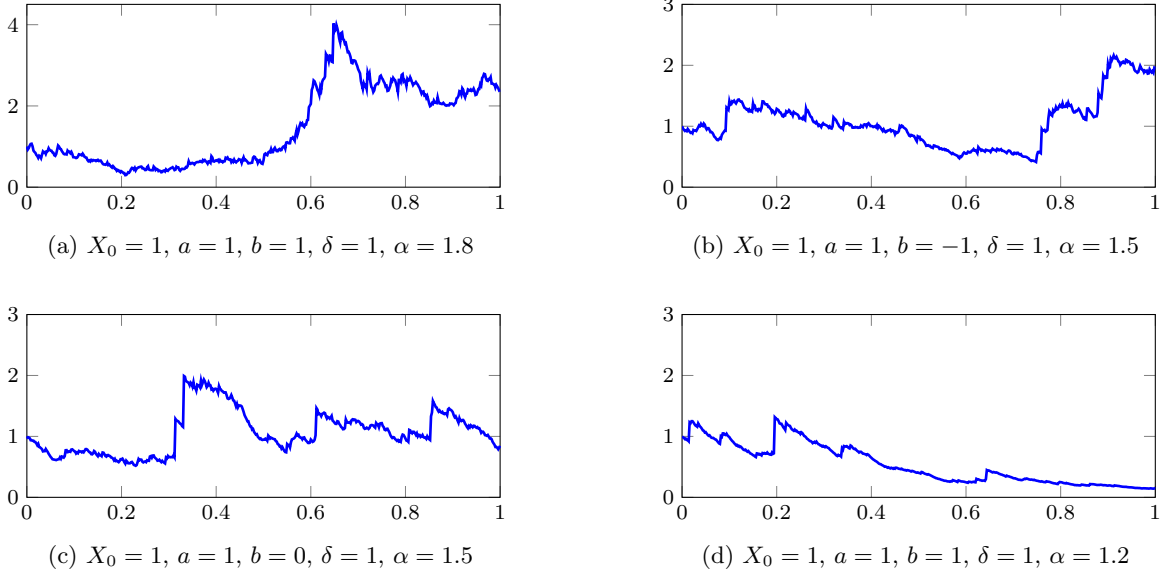


Fig 1: Simulation of trajectories of the α -CIR process

where

$$B_{\alpha,\beta} = \frac{\arctan(\beta \tan \frac{\alpha\pi}{2})}{\alpha}, \quad S_{\alpha,\beta} = \left(1 + \beta^2 \tan^2 \frac{\alpha\pi}{2}\right)^{1/(2\alpha)}. \quad (1.5)$$

In this paper, we will consider α -stable variables with $\beta = 1$, $\alpha \in (1, 2)$.

Using independent uniform and exponential random variables, we are now able to simulate independent copies of $L_1^\alpha = L_1^{\alpha,1}$. We can now simulate the process $(X_t)_{t \in [0,1]}$ that solves (0.1) using the numerical scheme (1.1) with $H = +\infty$. For the rest of the simulations, we will consider high-frequency observations $(X_{\frac{i}{n}})_{1 \leq i \leq n}$. To have a more accurate simulation of our process, we use the numerical scheme with step $(1000n)^{-1}$. We show in Figure 1 some simulated trajectories for different parameter values.

2. Computing the density of a strictly α -stable process

To estimate the parameters, we use a quasi-likelihood method based on the density φ_α of a strictly α -stable random variable $L_1^\alpha = L_1^{\alpha,1}$. We now explain how to compute this density and its derivatives efficiently.

2.1. Density of a strictly α -stable process

The characteristic function of L_1^α has the following expression

$$\Phi^{\alpha,1}(z) = \mathbb{E} \left(e^{izL_1^\alpha} \right) = \exp \left(-|z|^\alpha \left(1 - i \tan \left(\frac{\pi\alpha}{2} \right) \operatorname{sgn}(z) \right) \right). \quad (2.1)$$

We could compute the density φ_α using a Fourier inversion of the characteristic function, but this would result in an integral on \mathbb{R} . We instead use the expression presented in Nolan [13], with an integral on a bounded interval which allows for an easy numerical computation of this density. In [13], Nolan gives a computation of the density of a α -stable random variable Y with characteristic function

$$\begin{aligned} \mathbb{E} \left(e^{izY} \right) &= \exp \left(-|z|^\alpha \left(1 + i\beta \tan \left(\frac{\pi\alpha}{2} \right) \operatorname{sgn}(z) (|z|^{1-\alpha} - 1) \right) \right) \\ &= \mathbb{E} \left(e^{iz(L_1^\alpha - \beta \tan(\frac{\pi\alpha}{2}))} \right). \end{aligned} \quad (2.2)$$

For such a random variable, and denoting by f its density function, the following representation holds :

$$f(x, \alpha, \beta) = \begin{cases} \frac{\alpha(x-\xi)^{1/(\alpha-1)}}{\pi|\alpha-1|} \int_{-B_{\alpha,\beta}}^{\pi/2} V(\theta, \alpha, \beta) \exp(-(x-\xi)^{\alpha/(\alpha-1)} V(\theta, \alpha, \beta)) d\theta & x > \xi \\ \frac{\Gamma(1+1/\alpha) \cos(B_{\alpha,\beta})}{\pi(1+\xi^2)^{1/(2\alpha)}} & x = \xi \\ f(-x, \alpha, -\beta) & x < \xi \end{cases} \quad (2.3)$$

where $\xi = -\beta \tan \frac{\pi\alpha}{2}$, $\Gamma(a) = \int_0^\infty x^{a-1} e^{-x} dx$, $B_{\alpha,\beta}$ is defined in (1.5) and

$$V(\theta, \alpha, \beta) = (\cos(\alpha B_{\alpha,\beta}))^{1/(\alpha-1)} \left(\frac{\cos \theta}{\sin(\alpha(\theta + B_{\alpha,\beta}))} \right)^{\alpha/(\alpha-1)} \frac{\cos(\alpha B_{\alpha,\beta} + (\alpha-1)\theta)}{\cos \theta}.$$

As highlighted by the characteristic functions (2.2) and (2.1), we have $Y = L_1^\alpha + \xi$. Hence, we get φ_α by

$$\varphi_\alpha(x) = f(x + \xi, \alpha, 1), \quad \forall x \in \mathbb{R}. \quad (2.4)$$

This density is available in the Python package Scipy [16] with the `scipy.stats.levy_stable` function, or in the R package `RStableDist` [18]. Figure 2 gives the graph of the density for different values of α .

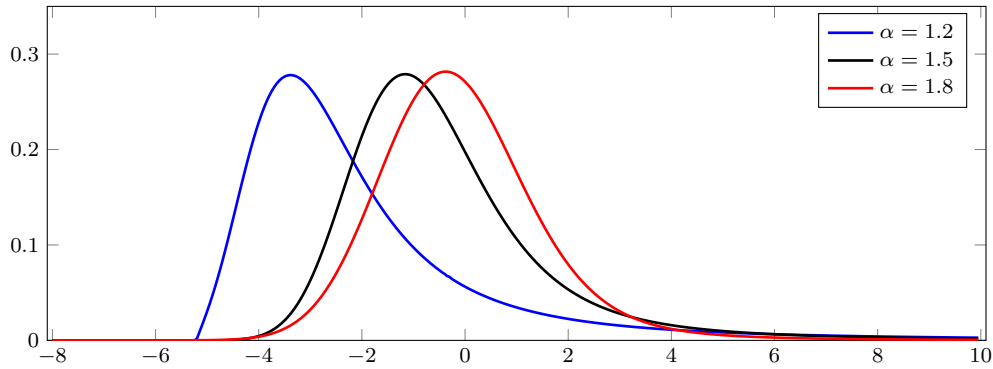


Fig 2: Graphs of the α -stable density φ_α ($\beta=1$) for different values of α

We can also check that this distribution is coherent with simulations done in Section 1.2. We generate independent copies of L_1^α according to equation (1.4) and compare the obtained distribution to the expected density as computed in (2.4). Figure 3 compares the density to the histogram of the obtained density when simulating $n = 100000$ independent copies of L_1^α .

For the rest of the simulations, we will use the scipy density because it has been optimised and makes the computations faster, but the explicit expression of the density is useful later when trying to compute the derivatives.

2.2. Derivatives of the density

The correction that we will apply to our first-step estimator uses the density φ_α and its derivatives. For symmetric α -stable distributions, a method for efficient evaluation of the derivatives of the density has been studied in Matsui and Tamekura [12]. Similarly to what is done for the symmetric process, we use the

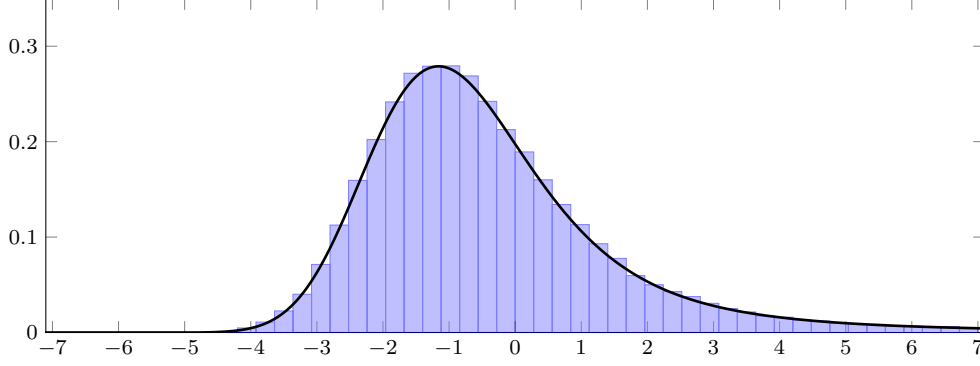


Fig 3: Distribution of simulated α -stable random variable ($\alpha = 1.5$, $\beta = 1$, $n = 100000$ variables) and comparison with the expected density φ_α

derivative of expression (2.3) to get the derivative with respect to x of the density. For $x > \xi$, we have

$$f'(x, \alpha, \beta) = \frac{\alpha x^{1/(\alpha-1)}}{\pi|\alpha-1|} \left(\frac{1}{x(\alpha-1)} \int_{-B_{\alpha,\beta}}^{\pi/2} V(\theta, \alpha, \beta) \exp(-x^{\alpha/(\alpha-1)} V(\theta, \alpha, \beta)) d\theta - \frac{\alpha}{\alpha-1} x^{1/(\alpha-1)} \int_{-B_{\alpha,\beta}}^{\pi/2} V(\theta, \alpha, \beta)^2 \exp(-x^{\alpha/(\alpha-1)} V(\theta, \alpha, \beta)) d\theta \right),$$

and for $x < \xi$

$$f'(x, \alpha, \beta) = -f'(-x, \alpha, -\beta).$$

We conclude using that

$$\varphi'_\alpha(x) = f'(x + \xi, \alpha, 1). \quad (2.5)$$

We confirm this expression of the derivative by comparing it to a two-point estimate and see that it agrees. In Figure 4, we give the graph of the derivative of the density for two values of α .

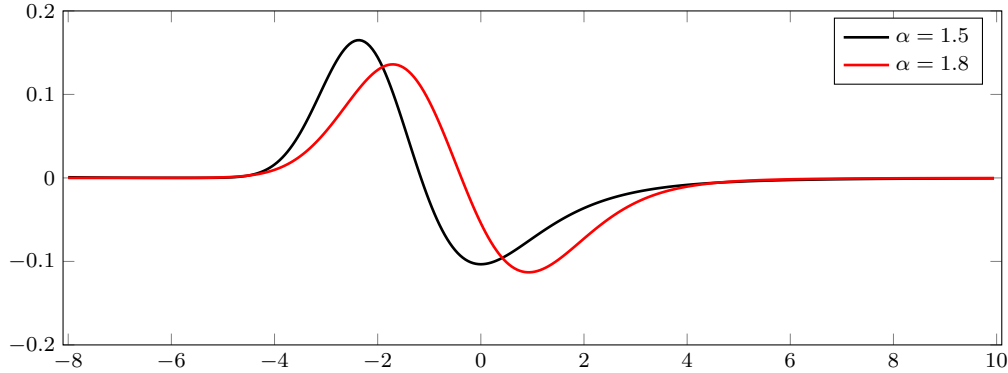


Fig 4: Graph of φ'_α for $\alpha_0 = 1.5$ and $\alpha_0 = 1.8$

However, contrary to the symmetric case, the bound of the integral given by the $B_{\alpha,\beta}$ parameter defined in (1.5) depends on α . This makes the exact computation of $\partial_\alpha \varphi$ too costly, and leads in practice to very unstable results. We therefore use a two-point estimate

$$\partial_\alpha \varphi(x, \alpha) = \frac{\varphi(x, \alpha + h) - \varphi(x, \alpha - h)}{2h}.$$

3. Monte-Carlo estimators

3.1. Estimation method

This paper is a follow-up to the previous article [1] in which we propose estimators of the parameter $\theta = (a, b, \delta, \alpha)$ and study their asymptotic properties. Following [1] we propose a first-step estimator, which is fairly easy to compute but is not rate optimal. This estimator will then be corrected to reach an efficient estimator.

We first estimate the jump activity coefficient α_0 by the power variation method described in Todorov [15]

$$\tilde{\alpha}_n = \frac{\log 2}{2 \log(V_n^2(1/2, X)/V_n^1(1/2, X))} \mathbb{1}_{V_n^1(1/2, X) \neq V_n^2(1/2, X)} \quad (3.1)$$

where

$$V_n^1(p, X) = \sum_{i=2}^n |\Delta_i^n X - \Delta_{i-1}^n X|^p \quad \text{with } \Delta_i^n X = X_{\frac{i}{n}} - X_{\frac{i-1}{n}},$$

$$V_n^2(p, X) = \sum_{i=4}^n |\Delta_i^n X - \Delta_{i-1}^n X + \Delta_{i-2}^n X - \Delta_{i-3}^n X|^p.$$

This estimator is easy and quick to compute numerically.

The scaling parameter δ_0 is next estimated, using again a power-variation method

$$\tilde{\delta}_n = \left(\frac{1}{m_{1/2}(\tilde{\alpha}_n)} \frac{1}{n} \sum_{i=2}^n n^{1/2\tilde{\alpha}_n} \frac{|X_{\frac{i}{n}} - 2X_{\frac{i-1}{n}} + X_{\frac{i-2}{n}}|^{1/2}}{X_{\frac{i-2}{n}}^{1/2\tilde{\alpha}_n}} \right)^2 \quad (3.2)$$

with $m_{1/2}(\alpha) = \mathbb{E}(|2^{1/\alpha} S_1^\alpha|^{1/2})$ where S_1^α has a symmetric α -stable distribution. From Masuda [9], we have $\forall q \in (-1, \alpha)$, $\mathbb{E}|S_1^\alpha|^q = \frac{2^q \Gamma(\frac{q+1}{2}) \Gamma(1-\frac{q}{\alpha})}{\sqrt{\pi} \Gamma(1-\frac{q}{2})}$. Hence $m_{1/2}(\tilde{\alpha}_n)$ is easy to compute, and so is $\tilde{\delta}_n$.

To estimate the drift parameters (a, b) , we consider the quasi-likelihood function given by (recalling that $\theta = (a, b, \delta, \alpha)$)

$$L_n(\theta) = \sum_{i=1}^n \log \left(\frac{n^{1/\alpha}}{\delta X_{\frac{i-1}{n}}^{1/\alpha}} \varphi_\alpha(z_i^n(\theta)) \right) \quad \text{with } z_i^n(\theta) = n^{1/\alpha} \frac{X_{\frac{i}{n}} - X_{\frac{i-1}{n}} - \frac{a}{n} + \frac{b}{n} X_{\frac{i-1}{n}}}{\delta X_{\frac{i-1}{n}}^{1/\alpha}}. \quad (3.3)$$

When δ_0 and α_0 are known, we maximise the quasi-likelihood function $(a, b) \rightarrow L_n(a, b, \delta_0, \alpha_0)$ to build the estimators of the drift (\hat{a}_n, \hat{b}_n) . Similarly, when α_0 and δ_0 are estimated by $\tilde{\alpha}_n$ and $\tilde{\delta}_n$, we maximise $(a, b) \rightarrow L_n(a, b, \tilde{\delta}_n, \tilde{\alpha}_n)$ and we denote by $(\tilde{a}_n, \tilde{b}_n)$ the resulting estimators.

We introduce the notations $h_\alpha(x) = \frac{\varphi'_\alpha}{\varphi_\alpha}(x)$, $k_\alpha(x) = 1 + x h_\alpha(x)$, $f_\alpha(x) = \frac{\partial_\alpha \varphi_\alpha}{\varphi_\alpha}(x)$ and

$$I^{11}(\theta) = \left(\begin{array}{cc} \frac{1}{\delta^2} \int_0^1 \frac{1}{X_s^{2/\alpha}} ds \mathbb{E}(h_\alpha^2(L_1)) & \frac{-1}{\delta^2} \int_0^1 \frac{X_s}{X_s^{2/\alpha}} ds \mathbb{E}(h_\alpha^2(L_1)) \\ \frac{-1}{\delta^2} \int_0^1 \frac{X_s}{X_s^{2/\alpha}} ds \mathbb{E}(h_\alpha^2(L_1)) & \frac{1}{\delta^2} \int_0^1 \frac{X_s^2}{X_s^{2/\alpha}} ds \mathbb{E}(h_\alpha^2(L_1)) \end{array} \right). \quad (3.4)$$

We summarise in the next result the asymptotic properties of these estimators.

Theorem 3.1. (i) $\tilde{\alpha}_n$ given by (3.1) converges in probability to α_0 and $\sqrt{n}(\tilde{\alpha}_n - \alpha_0)$ stably converges in law.

(ii) $\tilde{\delta}_n$ given by (3.2) converges in probability to δ_0 and $\frac{\sqrt{n}}{\ln(n)}(\tilde{\delta}_n - \delta_0)$ is tight.

(iii) For α_0 and δ_0 known, we have the stable convergence in law

$$n^{1/\alpha_0-1/2} \begin{pmatrix} \hat{a}_n - a_0 \\ \hat{b}_n - b_0 \end{pmatrix} \xrightarrow[n \rightarrow \infty]{\mathcal{L}-s} I^{11}(\theta_0)^{-1/2} \mathcal{N} \quad (3.5)$$

where \mathcal{N} is a standard Gaussian variable independent of $I^{11}(\theta_0)$.

(iv) For $\tilde{\alpha}_n$ and $\tilde{\delta}_n$ estimating α_0 and δ_0 , $\frac{n^{1/\alpha_0-1/2}}{\ln(n)^2} \begin{pmatrix} \tilde{\alpha}_n - \alpha_0 \\ \tilde{\delta}_n - \delta_0 \end{pmatrix}$ is tight.

(i) is proven in Todorov [15]. (ii) is proven in Theorem 4.3 of [1]. (iii) and (iv) are proven in Theorem 4.2 of [1].

We compute a preliminary estimator by successively estimating $\tilde{\alpha}_n$ from (3.1) and $\tilde{\delta}_n$ from (3.2). Then, we estimate the drift parameters (a, b) by maximising the quasi-likelihood function restricted to the drift $(a, b) \rightarrow L_n(a, b, \tilde{\delta}_n, \tilde{\alpha}_n)$ with L_n defined in (3.3) and we denote by $(\tilde{a}_n, \tilde{b}_n)$ the resulting estimators. We obtain a preliminary estimator $\hat{\theta}_{0,n} = (\tilde{a}_n, \tilde{b}_n, \tilde{\delta}_n, \tilde{\alpha}_n)$. For Theorem 3.1 this estimator is consistent but not rate optimal as we only prove the tightness of $\ln(n)^{-2} u_n^{-1}(\hat{\theta}_{0,n} - \theta_0)$, where

$$u_n^{-1} = \begin{pmatrix} n^{1/\alpha_0-1/2} \text{Id}_2 & 0 \\ 0 & \sqrt{n} \begin{pmatrix} \frac{1}{\delta_0} & \frac{\ln(n)}{\alpha_0^2} \\ 0 & 1 \end{pmatrix} \end{pmatrix}, \quad \text{Id}_2 = \begin{pmatrix} 1 & 0 \\ 0 & 1 \end{pmatrix}. \quad (3.6)$$

We correct this non-efficient preliminary estimator $\hat{\theta}_{0,n}$ with a one-step procedure :

$$\hat{\theta}_{1,n} = \hat{\theta}_{0,n} - J_n(\hat{\theta}_{0,n})^{-1} G_n(\hat{\theta}_{0,n}), \quad (3.7)$$

where $G_n = -\nabla_{\theta} \log L_n(\theta)$ and $J_n = \nabla_{\theta} G_n$. We define

$$I(\theta) = \begin{pmatrix} I^{11}(\theta) & (I^{21}(\theta))^T \\ I^{21}(\theta) & I^{22}(\theta) \end{pmatrix} \quad (3.8)$$

where $I^{11}(\theta)$ is defined in (3.4), $(I^{21}(\theta))^T$ denotes the transpose of $I^{21}(\theta)$ and

$$I^{21}(\theta) = \begin{pmatrix} \frac{1}{\delta} \int_0^1 \frac{ds}{X_s^{1/\alpha}} \mathbb{E}(h_{\alpha} k_{\alpha}(L_1^{\alpha})) & -\frac{1}{\delta} \int_0^1 \frac{X_s}{X_s^{1/\alpha}} ds \mathbb{E}(h_{\alpha} k_{\alpha}(L_1^{\alpha})) \\ I_{21}^{21}(\theta) & I_{21}^{22}(\theta) \end{pmatrix}, \quad I^{22}(\theta) = \begin{pmatrix} \mathbb{E}(k_{\alpha}^2(L_1^{\alpha})) & I_{21}^{22}(\theta) \\ I_{21}^{22}(\theta) & I_{22}^{22}(\theta) \end{pmatrix}$$

where

$$\begin{aligned} I_{21}^{21}(\theta) &= -\frac{1}{\delta \alpha^2} \int_0^1 \frac{\ln(X_s)}{X_s^{1/\alpha}} ds \mathbb{E}(h_{\alpha} k_{\alpha}(L_1^{\alpha})) - \frac{1}{\delta} \int_0^1 \frac{ds}{X_s^{1/\alpha}} \mathbb{E}(f_{\alpha} h_{\alpha}(L_1^{\alpha})) \\ I_{22}^{21}(\theta) &= \frac{1}{\delta \alpha^2} \int_0^1 \frac{\ln(X_s) X_s}{X_s^{1/\alpha}} ds \mathbb{E}(h_{\alpha} k_{\alpha}(L_1^{\alpha})) + \frac{1}{\delta} \int_0^1 \frac{X_s}{X_s^{1/\alpha}} ds \mathbb{E}(f_{\alpha} h_{\alpha}(L_1^{\alpha})) \\ I_{21}^{22}(\theta) &= -\frac{1}{\alpha^2} \int_0^1 \ln(X_s) ds \mathbb{E}(k_{\alpha}^2(L_1^{\alpha})) - \mathbb{E}(f_{\alpha} k_{\alpha}(L_1^{\alpha})) \\ I_{22}^{22}(\theta) &= \frac{1}{\alpha^4} \int_0^1 \ln(X_s)^2 ds \mathbb{E}(k_{\alpha}^2(L_1^{\alpha})) + \frac{2}{\alpha^2} \int_0^1 \ln(X_s) ds \mathbb{E}(f_{\alpha} k_{\alpha}(L_1^{\alpha})) + \mathbb{E}(f_{\alpha}^2(L_1^{\alpha})). \end{aligned}$$

Corollary 3.1. *We have the stable convergence in law, with $I(\theta_0)$ defined in (3.8)*

$$u_n^{-1}(\hat{\theta}_{1,n} - \theta_0) \xrightarrow[n \rightarrow \infty]{\mathcal{L}-s} I(\theta_0)^{-1/2} \mathcal{N}. \quad (3.9)$$

This was proved in Corollary 4.1. of [1].

3.2. Simulation results for the first-step estimator

3.2.1. Estimation of α

In Table 1, we present results of numerical simulations conducted with the true value of the parameter $\alpha_0 = 1.3$. We let the number of data points n range in the set $\{128, 256, 512, 1024, 2048, 4096\}$. The process (X_t) is simulated according to the scheme (1.1) with step $(1000n)^{-1}$. We show a Monte-Carlo evaluation, based on $n_{MC} = 1000$ replications, for the mean and standard deviation of the estimator $\tilde{\alpha}_n$ given in (3.1).

| n | Mean of $\tilde{\alpha}_n$ | Standard deviation of $\tilde{\alpha}_n$ |
|------|----------------------------|--|
| 128 | 1.473 | $3.65 * 10^{-1}$ |
| 256 | 1.396 | $1.98 * 10^{-1}$ |
| 512 | 1.351 | $1.27 * 10^{-1}$ |
| 1024 | 1.333 | $8.88 * 10^{-2}$ |
| 2048 | 1.319 | $6.25 * 10^{-2}$ |
| 4096 | 1.310 | $4.65 * 10^{-2}$ |

TABLE 1. Mean and standard deviation of $\tilde{\alpha}_n$ with 1000 replications

3.2.2. Estimation of δ

In Tables 2-3, we present results of numerical simulations for the estimator $\tilde{\delta}_n$ given in (3.2) conducted with the true value of the parameter $\delta_0 = 1$, respectively for $\alpha_0 = 1.3$ known and for α_0 estimated by $\tilde{\alpha}_n$ as described in 3.2.1. We again let n range in the set $\{128, 256, 512, 1024, 2048, 4096\}$ and simulate (X_t) using (1.1) with step $(1000n)^{-1}$. We give an estimation by Monte-Carlo of the mean of the estimators together with their standard deviations. In these Monte-Carlo experiments, we used $n_{MC} = 1000$ replications. As expected, $\tilde{\delta}_n$ converges to δ_0 both when α_0 is known and when it is estimated, but the convergence is slower when α_0 is unknown and has to be estimated. This corresponds to the loss of rate $\ln(n)$ that happens when estimating δ and α simultaneously.

| n | Mean of $\tilde{\delta}_n$ | Std of $\tilde{\delta}_n$ |
|------|----------------------------|---------------------------|
| 128 | 0.944 | $2.10 * 10^{-1}$ |
| 256 | 0.967 | $1.41 * 10^{-1}$ |
| 512 | 0.983 | $1.07 * 10^{-1}$ |
| 1024 | 0.988 | $7.60 * 10^{-2}$ |
| 2048 | 0.994 | $5.44 * 10^{-2}$ |
| 4096 | 0.998 | $3.92 * 10^{-2}$ |

TABLE 2. Mean and standard deviation of $\tilde{\delta}_n$ for $\alpha_0 = 1.3$ known with 1000 replications

| n | Mean of $\tilde{\delta}_n$ | Std of $\tilde{\delta}_n$ |
|------|----------------------------|---------------------------|
| 128 | 0.859 | $4.93 * 10^{-1}$ |
| 256 | 0.899 | $3.79 * 10^{-1}$ |
| 512 | 0.932 | $3.52 * 10^{-1}$ |
| 1024 | 0.941 | $2.89 * 10^{-1}$ |
| 2048 | 0.959 | $2.31 * 10^{-1}$ |
| 4096 | 0.978 | $1.94 * 10^{-1}$ |

TABLE 3. Mean and standard deviation of $\tilde{\delta}_n$ for $\tilde{\alpha}_n$ estimating α_0 with 1000 replications

3.2.3. Estimation of the drift for δ_0 and α_0 known

To have an idea of what the quasi-likelihood function (3.3) looks like, we simulate one sample path of observations $(X_{\frac{i}{n}})_{i=0, \dots, n}$ with $n = 1000$, $a_0 = 3$, $b_0 = 5$, $\delta_0 = 1$ and $\alpha_0 = 1.3$, and we plot in Figure 5 the graph of

$$\begin{aligned} [0.5, 5] \times [3, 8] &\rightarrow \mathbb{R} \\ (a, b) &\rightarrow L_n(a, b, \delta_0, \alpha_0). \end{aligned}$$

This quasi-likelihood function is concave. We see that the maximum in (a, b) is reached near the true value (a_0, b_0) . Maximising with respect to the two parameters using the Python Scipy package, we get $(\hat{a}_n, \hat{b}_n) = (3.047, 5.068)$. We can see that there is an area where the quasi-likelihood doesn't vary much. This can lead to difficulties when maximising it, especially later for estimated values of δ and α .

The maximisation of L_n is conducted using quasi-Newton methods implemented in Python Scipy package. It necessitates to compute numerically the values of the quasi-likelihood function as detailed in Section 2, and thus involves the numerous evaluations of $(\varphi_\alpha(z_i^n(\theta)))_{i=1, \dots, n}$. To make the estimation faster, these

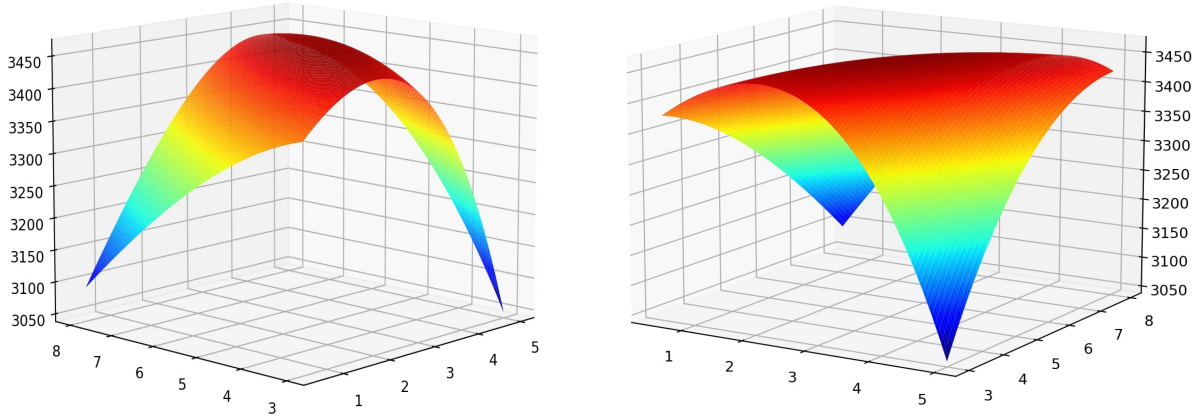


Fig 5: Views of the quasi-likelihood

computations can be parallelised using the Python package Joblib.

In order to check the convergence (3.5), in which the asymptotic law is conditionally Gaussian, we will check that for $\Sigma = I^{11}(\theta_0)^{-1}$

$$n^{1/\alpha_0-1/2}(\hat{a}_n - a_0) \xrightarrow[n \rightarrow \infty]{\mathcal{L}-s} \sqrt{\Sigma_{11}}\mathcal{N} \quad \text{and} \quad n^{1/\alpha_0-1/2}(\hat{b}_n - b_0) \xrightarrow[n \rightarrow \infty]{\mathcal{L}-s} \sqrt{\Sigma_{22}}\mathcal{N}.$$

We estimate Σ by $\Sigma_n = I_n^{11}(\theta_0)^{-1}$ with

$$I_n^{11}(\theta_0) = \frac{1}{n} \sum_{i=1}^n \begin{pmatrix} \frac{1}{\delta_0^2} \frac{1}{X_{i-1}^{2/\alpha_0}} \mathbb{E}(h_{\alpha_0}^2(L_1^{\alpha_0})) & \frac{-1}{\delta_0^2} \frac{X_{i-1}}{X_{i-1}^{2/\alpha_0}} \mathbb{E}(h_{\alpha_0}^2(L_1^{\alpha_0})) \\ \frac{-1}{\delta_0^2} \frac{X_{i-1}}{X_{i-1}^{2/\alpha_0}} \mathbb{E}(h_{\alpha_0}^2(L_1^{\alpha_0})) & \frac{1}{\delta_0^2} \frac{X_{i-1}^2}{X_{i-1}^{2/\alpha_0}} \mathbb{E}(h_{\alpha_0}^2(L_1^{\alpha_0})) \end{pmatrix}$$

where $\mathbb{E}(h_{\alpha_0}^2(L_1^{\alpha_0}))$ is calibrated once with a Monte-Carlo method with a very large $n_{MC} = 100000$. The proof of Theorem 3.1. in [1] shows that $I_n^{11}(\theta_0)$ converges in probability to $I^{11}(\theta_0) > 0$ which allows us to conclude

$$((\Sigma_n)_{11})^{-1/2} n^{1/\alpha_0-1/2}(\hat{a}_n - a_0) \xrightarrow[n \rightarrow \infty]{\mathcal{L}} \mathcal{N} \quad \text{and} \quad ((\Sigma_n)_{22})^{-1/2} n^{1/\alpha_0-1/2}(\hat{b}_n - b_0) \xrightarrow[n \rightarrow \infty]{\mathcal{L}} \mathcal{N}.$$

| n | Mean of \hat{a}_n | Std of \hat{a}_n | Mean of \hat{b}_n | Std of \hat{b}_n |
|------|---------------------|--------------------|---------------------|--------------------|
| 128 | 3.064 | $4.25 * 10^{-1}$ | 4.633 | $5.61 * 10^{-1}$ |
| 256 | 3.056 | $3.53 * 10^{-1}$ | 4.779 | $4.64 * 10^{-1}$ |
| 512 | 3.056 | $2.86 * 10^{-1}$ | 4.895 | $4.10 * 10^{-1}$ |
| 1024 | 3.038 | $2.44 * 10^{-1}$ | 4.929 | $3.24 * 10^{-1}$ |
| 2048 | 3.029 | $2.08 * 10^{-1}$ | 4.976 | $2.84 * 10^{-1}$ |
| 4096 | 3.024 | $1.69 * 10^{-1}$ | 4.981 | $2.37 * 10^{-1}$ |

TABLE 4. Mean and standard deviation of the drift estimators with $\delta_0 = 1$ and $\alpha_0 = 1.3$ known, with 1000 replications

From Table 4, we see that assuming δ_0 and α_0 known the joint estimation of drift parameters works well, but with a relatively slow rate of convergence $n^{1/\alpha_0-1/2}$. Hence this estimation works better for a value of α_0 closer to 1. This is also highlighted by Figure 6, where the convergence is a lot quicker for $\alpha_0 = 1.1$ where $n^{1/\alpha_0-1/2} \approx n^{0.41}$, than for $\alpha_0 = 1.3$ where $n^{1/\alpha_0-1/2} \approx n^{0.27}$.

In Table 5, we see that the asymptotic behaviour of the estimator is as predicted from the theoretical study, the rate of estimation for (\hat{a}_n, \hat{b}_n) is $n^{1/\alpha_0-1/2}$ and the asymptotic rescaled standard deviations are very close to the theoretical one.

In Figure 7, we plot the distributions of the rescaled errors of estimation together with their Gaussian limits. We see that the empirical distributions fit very well the theoretical ones.

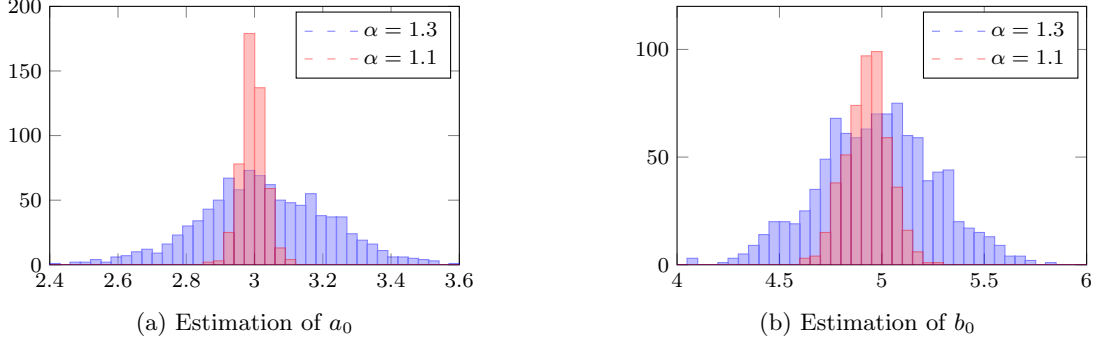


Fig 6: Impact of α_0 on the convergence of the drift ($a_0 = 3$, $b_0 = 5$, $\delta_0 = 1$, $n=2048$)

| n | $((\Sigma_n)_{11})^{-1/2} n^{1/\alpha_0 - 1/2} (\hat{a}_n - a_0)$ | | $((\Sigma_n)_{22})^{-1/2} n^{1/\alpha_0 - 1/2} (\hat{b}_n - b_0)$ | |
|-------------------|---|-------|---|-------|
| | Mean | Std | Mean | Std |
| 128 | $7.86 * 10^{-2}$ | 0.954 | $-6.54 * 10^{-1}$ | 0.946 |
| 256 | $9.75 * 10^{-2}$ | 0.959 | $-4.75 * 10^{-1}$ | 0.937 |
| 512 | $1.52 * 10^{-1}$ | 0.983 | $-2.75 * 10^{-1}$ | 0.982 |
| 1024 | $1.25 * 10^{-1}$ | 0.985 | $-2.32 * 10^{-1}$ | 0.946 |
| 2048 | $1.34 * 10^{-1}$ | 0.964 | $-1.04 * 10^{-1}$ | 0.998 |
| 4096 | $1.20 * 10^{-2}$ | 0.972 | $-9.34 * 10^{-2}$ | 0.988 |
| Theoretical limit | 0 | 1 | 0 | 1 |

TABLE 5. Mean and standard deviation of the rescaled errors

3.3. Simulation results for the one-step correction

In the following, we aim to show that the joint estimation of $\theta = (a, \delta, \alpha)$ is feasible in practice, assuming $b_0 = 5$ known, and that the one-step improvement leads to a rate-efficient estimator. The gradient and Hessian of the quasi-likelihood function G_n and J_n will be computed using finite differences, for reasons explained in Section 2.2. For this estimation, the theoretical variance is $\bar{\Sigma} = \bar{I}(\theta_0)^{-1}$ with

$$\bar{I}(\theta_0) = \begin{pmatrix} \frac{1}{\delta_0^2} \int_0^1 \frac{1}{X_s^{2/\alpha_0}} ds \mathbb{E}(h_{\alpha_0}^2(L_1^{\alpha_0})) & \frac{1}{\delta_0} \int_0^1 \frac{ds}{X_s^{1/\alpha_0}} \mathbb{E}(h_{\alpha_0} k_{\alpha_0}(L_1^{\alpha_0})) & I_{21}^{21}(\theta) \\ \frac{1}{\delta_0} \int_0^1 \frac{ds}{X_s^{1/\alpha_0}} \mathbb{E}(h_{\alpha_0} k_{\alpha_0}(L_1^{\alpha_0})) & \mathbb{E}(k_{\alpha_0}^2(L_1^{\alpha_0})) & I_{21}^{22}(\theta) \\ I_{21}^{21}(\theta) & I_{21}^{22}(\theta) & I_{22}^{22}(\theta) \end{pmatrix}$$

the restriction of $I(\theta_0)$ (defined in (3.8)) to the estimation of (a, δ, α) . We estimate $\bar{\Sigma} = \bar{I}(\theta_0)^{-1}$ by $\bar{\Sigma}_n = \bar{I}_n^{-1}$ where the integrals are estimated by Riemann sums, and the expectations are calibrated once with a Monte-Carlo method with a very large $n_{MC} = 100000$. For instance

$$(\bar{I}_n(\theta_0))_{11} = \frac{1}{\delta_0^2} \frac{1}{n} \sum_{i=1}^n \frac{1}{X_{\frac{i-1}{n}}^{2/\alpha_0}} \mathbb{E}(h_{\alpha_0}^2(L_1^{\alpha_0})).$$

We have proved in [1] that $\bar{I}_n(\theta_0)$ converges in probability to $\bar{I}(\theta_0) > 0$. Hence from (3.8) we have the convergences in law

$$\begin{aligned} ((\bar{\Sigma}_n)_{11})^{-1/2} n^{1/\alpha_0 - 1/2} (\hat{a}_{1,n} - a_0) &\xrightarrow[n \rightarrow \infty]{\mathcal{L}-s} \mathcal{N}, \\ ((\bar{\Sigma}_n)_{33})^{-1/2} \frac{\sqrt{n}}{\ln(n)} \frac{\alpha_0^2}{\delta_0} (\hat{\delta}_{1,n} - \delta_0) &\xrightarrow[n \rightarrow \infty]{\mathcal{L}-s} \mathcal{N}, \\ ((\bar{\Sigma}_n)_{33})^{-1/2} \sqrt{n} (\hat{\alpha}_{1,n} - \alpha_0) &\xrightarrow[n \rightarrow \infty]{\mathcal{L}-s} \mathcal{N}. \end{aligned}$$

We consider larger values of n than we did previously, as smaller values such as $n = 512$ lead to mixed results. We have once again simulated the process (X_t) using the scheme described in (1.1) with step $(1000n)^{-1}$.

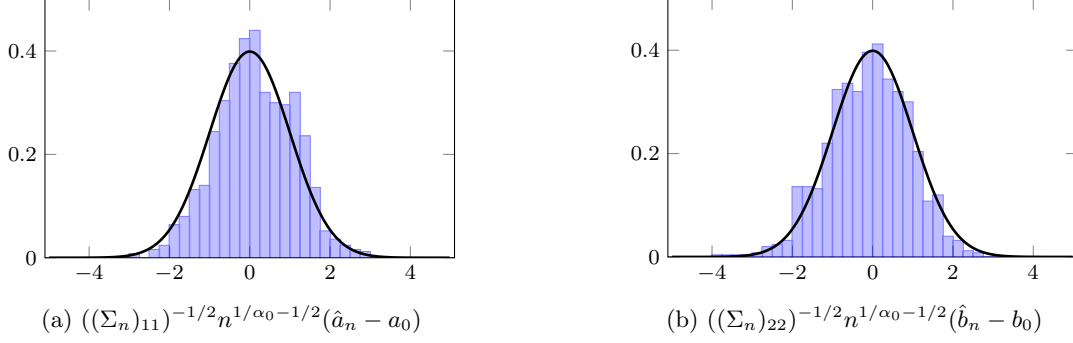


Fig 7: Distribution of the rescaled errors of estimation and comparison with $\mathcal{N}(0, 1)$
 $(a_0 = 3, b_0 = 5, \delta_0 = 1, \alpha_0 = 1.3, n = 2048)$

For these simulations, we chose $a_0 = 3, b_0 = 5, \delta_0 = 1$ and $\alpha_0 = 1.3$. The following results are obtained with $n_{MC} = 1000$ replications.

From Tables 6 and 7, we can check the impact of the one-step improvement. While the mean converges and the standard deviation decreases as n increases for both the preliminary and corrected estimators, we can see that the corrected estimators have much lower standard deviations. This significant improvement is also very clear in Figure 8. While both estimators are centered around the true value of the parameters, the lower variance of the one-step estimator leads to a more accurate estimation.

| n | Mean of \tilde{a}_n | Mean of $\hat{a}_{1,n}$ | Mean of $\tilde{\delta}_n$ | Mean of $\hat{\delta}_{1,n}$ | Mean of $\tilde{\alpha}_n$ | Mean of $\hat{\alpha}_{1,n}$ |
|------|-----------------------|-------------------------|----------------------------|------------------------------|----------------------------|------------------------------|
| 2048 | 3.017 | 2.854 | 0.948 | 0.984 | 1.322 | 1.289 |
| 4096 | 3.011 | 2.913 | 0.962 | 0.989 | 1.314 | 1.294 |
| 8192 | 3.020 | 2.932 | 0.976 | 0.991 | 1.307 | 1.298 |

TABLE 6. Mean of the estimators before and after correction, with 1000 replications

| n | Std of \tilde{a}_n | Std of $\hat{a}_{1,n}$ | Std of $\tilde{\delta}_n$ | Std of $\hat{\delta}_{1,n}$ | Std of $\tilde{\alpha}_n$ | Std of $\hat{\alpha}_{1,n}$ |
|------|----------------------|------------------------|---------------------------|-----------------------------|---------------------------|-----------------------------|
| 2048 | 1.15 | 0.875 | $2.22 * 10^{-1}$ | $1.19 * 10^{-1}$ | $6.18 * 10^{-2}$ | $4.43 * 10^{-2}$ |
| 4096 | $7.99 * 10^{-1}$ | $5.27 * 10^{-1}$ | $1.87 * 10^{-1}$ | $7.55 * 10^{-2}$ | $4.67 * 10^{-2}$ | $2.24 * 10^{-2}$ |
| 8192 | $8.45 * 10^{-1}$ | $4.37 * 10^{-1}$ | $1.44 * 10^{-1}$ | $5.07 * 10^{-2}$ | $3.16 * 10^{-2}$ | $1.21 * 10^{-2}$ |

TABLE 7. Standard deviation of the estimators before and after correction, with 1000 replications

In Figure 9, we plot the distributions of the rescaled errors of estimation of the one-step estimator, together with the standard Gaussian. We see that the empirical distributions of the one-step estimator fit the theoretical ones.

Remark 3.1. When estimating α in Section 3.2.1, we already had a rate of convergence \sqrt{n} , which is the same as the efficient rate. The improvement visible in Figure 8 comes from the better variance. This is also true for the estimation of δ . On the other hand, the estimation of the drift gains in rate with this improvement.

Remark 3.2. We also know from Section 5.6. in [1] that, for some neighbourhood of θ_0 $V_n^{(\eta)}$,

$$\sup_{\theta \in V_n^{(\eta)}} \left\| u_n^T J_n(\theta) u_n - I(\theta_0) \right\| \rightarrow 0.$$

So we could try using $(u_n^T)^{-1} I(\hat{\theta}_{0,n}) u_n^{-1}$ instead of $J_n(\hat{\theta}_{0,n})$ in our one-step procedure. However, numerical computations show similar results in both cases. Moreover, we would need to estimate $I(\hat{\theta}_{0,n})$ by $I_n(\hat{\theta}_{0,n})$

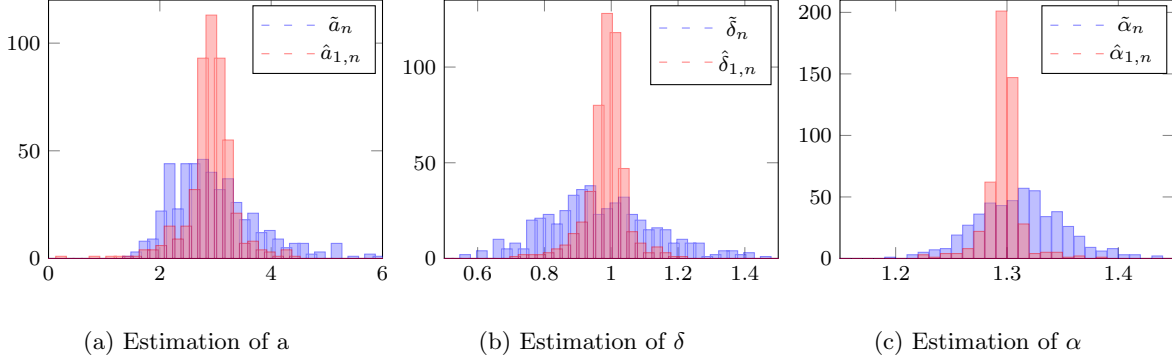


Fig 8: Distribution of estimation before and after one-step improvement
 $(a_0 = 3, b_0 = 5, \delta_0 = 1, \alpha_0 = 1.3, n = 5000)$

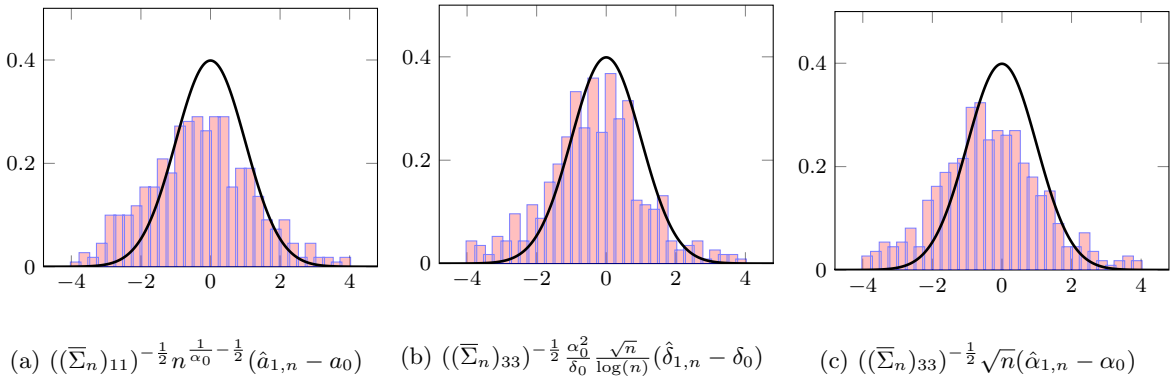


Fig 9: Distribution of the rescaled errors of estimation after the one-step improvement, and comparison with $\mathcal{N}(0, 1)$ ($a_0 = 3, b_0 = 5, \delta_0 = 1, \alpha_0 = 1.3, n = 5000$)

using Riemann sums to estimate the integrals and to compute the expectations, for instance $\mathbb{E}(h_{\hat{\alpha}_n}(L_1^{\hat{\alpha}_n}))$. As the matrix $I_n(\hat{\theta}_{0,n})$ is full, the resulting Monte-Carlo simulation drastically slows down the estimation. In conclusion, this method would be significantly longer for similar results.

However, this method would be worth considering when working with a symmetric stable process S^α such as in Brouste and Masuda [2]. In this case a lot of terms in the matrix $I_n(\hat{\theta}_{0,n})$ are 0, leaving us with only a few expectations to compute which makes this technique viable.

References

- [1] Elise Bayraktar and Emmanuelle Clément. Estimation of a pure-jump stable Cox-Ingersoll-Ross process. To appear in Bernoulli hal-04037024, 2023.
- [2] Alexandre Brouste and Hiroki Masuda. Efficient estimation of stable Lévy process with symmetric jumps. *Stat. Inference Stoch. Process.*, 21(2):289–307, 2018.
- [3] Emmanuelle Clément and Arnaud Gloter. Joint estimation for SDE driven by locally stable Lévy processes. *Electron. J. Stat.*, 14(2):2922–2956, 2020.
- [4] John C. Cox, Jonathan E. Ingersoll, Jr., and Stephen A. Ross. A theory of the term structure of interest rates. *Econometrica*, 53(2):385–407, 1985.
- [5] Zongfei Fu and Zenghu Li. Stochastic equations of non-negative processes with jumps. *Stochastic Process. Appl.*, 120(3):306–330, 2010.
- [6] Ying Jiao, Chunhua Ma, and Simone Scotti. Alpha-CIR model with branching processes in sovereign interest rate modeling. *Finance Stoch.*, 21(3):789–813, 2017.

- [7] Ying Jiao, Chunhua Ma, Simone Scotti, and Chao Zhou. The alpha-Heston stochastic volatility model. *Math. Finance*, 31(3):943–978, 2021.
- [8] Libo Li and Dai Taguchi. On a positivity preserving numerical scheme for jump-extended CIR process: the alpha-stable case. *BIT*, 59(3):747–774, 2019.
- [9] Hiroki Masuda. Joint estimation of discretely observed stable Lévy processes with symmetric Lévy density. *J. Japan Statist. Soc.*, 39(1):49–75, 2009.
- [10] Hiroki Masuda. Non-Gaussian quasi-likelihood estimation of SDE driven by locally stable Lévy process. *Stochastic Process. Appl.*, 129(3):1013–1059, 2019.
- [11] Hiroki Masuda. Optimal stable Ornstein-Uhlenbeck regression. *Jpn. J. Stat. Data Sci.*, 6(1):573–605, 2023.
- [12] Muneya Matsui and Akimichi Takemura. Some improvements in numerical evaluation of symmetric stable density and its derivatives. *Comm. Statist. Theory Methods*, 35(1-3):149–172, 2006.
- [13] John P. Nolan. Numerical calculation of stable densities and distribution functions. *Comm. Statist. Stochastic Models*, 13(4):759–774, 1997.
- [14] Ken-iti Sato. *Lévy processes and infinitely divisible distributions*, volume 68 of *Cambridge Studies in Advanced Mathematics*. Cambridge University Press, Cambridge, 2013. Translated from the 1990 Japanese original, Revised edition of the 1999 English translation.
- [15] Viktor Todorov. Power variation from second order differences for pure jump semimartingales. *Stochastic Process. Appl.*, 123(7):2829–2850, 2013.
- [16] Pauli Virtanen, Ralf Gommers, Travis E. Oliphant, Matt Haberland, Tyler Reddy, David Cournapeau, Evgeni Burovski, Pearu Peterson, Warren Weckesser, Jonathan Bright, Stéfan J. van der Walt, Matthew Brett, Joshua Wilson, K. Jarrod Millman, Nikolay Mayorov, Andrew R. J. Nelson, Eric Jones, Robert Kern, Eric Larson, C J Carey, İlhan Polat, Yu Feng, Eric W. Moore, Jake VanderPlas, Denis Laxalde, Josef Perktold, Robert Cimrman, Ian Henriksen, E. A. Quintero, Charles R. Harris, Anne M. Archibald, Antônio H. Ribeiro, Fabian Pedregosa, Paul van Mulbregt, and SciPy 1.0 Contributors. SciPy 1.0: Fundamental Algorithms for Scientific Computing in Python. *Nature Methods*, 17:261–272, 2020.
- [17] Aleksander Weron and Rafał Weron. Computer simulation of Lévy α -stable variables and processes. In *Chaos—the interplay between stochastic and deterministic behaviour (Karpacz, 1995)*, volume 457 of *Lecture Notes in Phys.*, pages 379–392. Springer, Berlin, 1995.
- [18] Diethelm Wuertz, Martin Maechler, and Rmetrics core team members. *stabledist: Stable Distribution Functions*, 2016. R package version 0.7-1.